6th European Conference on Computational Mechanics (ECCM 6)
7th European Conference on Computational Fluid Dynamics (ECFD 7)
11 – 15 June 2018, Glasgow, UK

# STATISTICAL MODELLING OF HDNR BEARING PROPERTIES VARIABILITY FOR THE SEISMIC RESPONSE OF ISOLATED STRUCTURES

**F. MICOZZI[1], L. RAGNI[2] AND A. DALL'ASTA[3]**

[1] University of Camerino - SAAD
Viale della Rimembranza, 63100, Ascoli Piceno
fabio.micozzi@unicam.it

[2] Marche Polytechnic University - DICEA
Via Brecce Bianche 12, 60131, Ancona
laura.ragni@univpm.it

[3]University of Camerino - SAAD
Viale della Rimembranza, 63100, Ascoli Piceno
andrea.dallasta@unicam.it

**Key words:** seismic isolation, HNDR bearings, material uncertainties, production variability.

**Abstract.** This paper reports some results of an ongoing Research Project called RINTC aimed at computing the risk of collapse of buildings conforming to the Italian Seismic Design Code. The project involves different areas of application (reinforced concrete, masonry, steel buildings, etc.) including reinforced concrete (RC) buildings equipped with isolation systems. In particular, this paper focuses on seismic isolation systems based on High Damping Natural Rubber (HDNR) bearings, which are widely employed for buildings and other structures. The aim of the paper is to evaluate the response dispersion due to the uncertainties in the seismic input as well as the variability of the isolation system properties. The study proposes a model to define the production variability of the bearing properties, taking into account the tolerance allowed in factory production control tests (FPCT) by the European code on anti-seismic devices (EN15129). To this purpose, in the first part of the paper, experimental results of groups of HDNR bearings belonging to different batches (classes) has been analysed, focusing on the values of shear stiffness and damping coefficient at design deformation and their correlation inside and between device groups. Both the intra-class and inter-class variability affecting the HDNR isolator properties are evaluated, by using a proper statistical model. Successively, the effect on the properties variability of the FPCT acceptance criteria provided by the European code is evaluated. In the second part of the paper, results of multi-stripe analyses carried out on a base isolated prototype consisting of a 6-storey RC building are presented for increasing ground motion intensities. In particular, several varied parameters of  bearings are sampled starting from mean properties and by using the statistical model calibrated from test data. The influence of the bearings parameters variability on the most interesting engineering demand parameters (EDPs) and on collapse modalities is evaluated and discussed.

## 1 INTRODUCTION

European regulation for anti-seismic devices EN15129 [1] defines criteria to identify the design properties (DP) of dissipation devices and isolation bearings and the allowed tolerance limits between these nominal values and the real characteristics of the produced devices (production variability) as well as the control testing procedures. For the elastomeric isolators, Type Testing (TT) described in section 8.2.4.1.2, defines nominal values of mechanical parameters to be used in structural design, while the Factory Production Control Testing (FPCT) reported in section 8.2.4.1.3 and related Table 11, defines tolerance limits of the production variability. In particular, the shear behaviour of elastomeric isolators (section 8.2) is described by the equivalent shear modulus $G$ and the equivalent damping coefficient $\xi$, measured at the third cycle of shear tests carried out at different deformation levels (section 8.2.1.2.2). A production variability of these two parameter equal to ±20% is allowed from the Code. It is also specified in section 8.2.4.1.4 that FPCT shall be carried out on at least 20% of the produced isolators, chosen randomly inside the batch.

The EN15129 also provides additional design recommendation, such as the upper and lower bound analyses approach. According with this recommendation, both the Upper Bound Design Properties (UBDP) and the Lower Bound Design Properties (LBDP), representing maximum and minimum values of the mechanical parameters obtained combining the different variability source, should be considered in the analyses of isolated structures. For example, regarding the production variability, nominal properties should be modified of ±20%, according to the acceptance criteria of the FPCT. Upper and lower bounds should be determined also for temperature and aging variations, combining the three source of variability with specific factors. The ratio between UBDP and LBDP shall be lower than 1.8 (section 8.2.1.1).

The Upper/Lower bound method is an effective and simple procedure to evaluate the effect of bearings properties variability on seismic performances of isolated structures; however it is a conservative approach. For this reason, a statistical model of the uncertainty relating to the bearing properties due to the production variability has been developed. The calibration of the model is based on experimental results of groups of specimens of HDR bearings belonging to different batches (classes). Successively, according with the statistical model, a sample generation procedure has been implemented taking into account also tolerance limits allowed by FPCT. Finally, the effect of the properties variability on the most interesting engineering demand parameters (EDPs) controlling the seismic performance as well as the collapse modalities has been assessed.

## 2 UNCERTAINTIES MODELLING OF THE ISOLATORS PROPERTIES

The Upper/Lower Bound method is an effective and simple procedure to evaluate the effect of bearings properties variability on seismic performances of isolated structures, but these variations do not represent the real variability of devices arising during the production process. In order to evaluate the effects of the isolator properties variability, a statistical model has been developed starting from experimental data. Finally, the effective variability expected in the seismic isolation system is obtained by combining, the statistical model describing the production variability with the simulation of the FPCT according to EN15129.

### 2.1 Statistical model

The statistical model chosen to describe the isolation-related uncertainties is the ANOVA model II (or *random* ANOVA model, [2]), where a population is divided in classes and classes have variable means but constant variances. According to ANOVA model II the $j^{th}$ value from the $i$ class can be expressed as follow

$$y_{ij} = \mu_{..} + \tau_{i.} + \varepsilon_{ij} \tag{1}$$

where $\mu_{..}$ is the overall mean (or *grand* mean), $\tau_{i.}$ is the deviation of the class mean $\mu_i$ from the grand mean and $\varepsilon_{ij}$ is the deviation of the $j^{th}$ value from the class mean $\mu_i$. The random variable $\tau_{i.}$ has a normal distribution with zero mean and variance $\sigma_B^2$ (between-class variance) while the random variable $\varepsilon_{ij}$ has a normal distribution with zero mean and variance $\sigma_w^2$ (within-class variance). The three parameters $\mu_{..}$, $\sigma_B^2$ and $\sigma_W^2$ fully define the statistical model.

In the case of seismic isolators, a variability inside each batch (class) is expected (within-class variability) as well as a variability between the mean values of each batch (between-class variability). Hereafter the procedure to estimate the parameters of the statistical model from data is shown, starting from the mean and the variance of each batch tested according to the FPCT. The grand mean $\mu_{..}$ of the sample is calculated as weighted mean of the batch means:

$$\mu_{..} = \overline{y_{..}} = \sum_{i=1}^{k} \frac{n_i}{n} \overline{y_{i.}} \tag{2}$$

where $\bar{y}_i$ is the mean of the $i^{th}$ batch, $n_i$ is the number of tested isolators belonging to the batch $i$, $n$ is the total number of the tested seismic isolators and $k$ is the number of batches. Table 1 summarizes the step to estimate the within-class variance ($\sigma_W^2$) and between-class variance ($\sigma_B^2$), where $s_i^2$ is the variance of the $i$ batch and $n'$ takes into account an unequal number of isolator inside each batch (unbalanced ANOVA) and is estimated as follows:

$$n' = \frac{1}{n-1}\left[\sum_{i=1}^{k} n_i - \sum_{i=1}^{k} n_i^2 \Big/ \sum_{i=1}^{k} n_i\right] \tag{3}$$

**Table 1**: ANOVA model II

| Sum of Squares | Degrees of freedom | Mean Squares (MS) | E(MS) |
|---|---|---|---|
| $SS_B = \sum_{i=1}^{k} n_i \left(\overline{y_{i.}} - \overline{y_{..}}\right)^2$ | $k-1$ | $MS_B = \frac{SS_B}{k-1}$ | $\sigma_W^2 + n'\sigma_B^2$ |
| $SS_W = \sum_{i=1}^{k}\sum_{j=1}^{n_i} n_i \left(y_{ij} - \overline{y_{i.}}\right)^2 = \sum_{i=1}^{k}(n_i - 1)s_i^2$ | $\sum_{i=1}^{k}(n_i - 1)$ | $MS_W = \frac{SS_W}{\sum_{i=1}^{k}(n_i - 1)}$ | $\sigma_W^2$ |

The overall variance is the sum of the within-class variance and the between-class variance

$$\sigma^2 = \sigma_W^2 + \sigma_B^2 \tag{4}$$

Finally the intra-class correlation is computed: it is a simple way to understand relative weight of the between-class variability and the within-class variability. It is define as the ratio of the between-class variance and the overall variance and can be estimated as follows:

$$IC = \frac{MS_B - MS_W}{MS_B + (n'-1)MS_W} \tag{5}$$

High *IC* indicates a relatively high between-class variability compared to the within-class one.

## 2.2 Calibration of the statistical model

A sample of 113 HDR bearings belonging to 30 different batches with different number of isolators is adopted to calibrate the statistical model described above. All the devices of the sample have a design property values $G$ = 0.4 N/mm$^2$ and $\xi$ = 15%, both measured at the 3$^{rd}$ cycle and at the design shear deformation $\gamma = 1.5$ .

First, the correlation between the shear modulus and the damping coefficient is calculated based on mean values of each batch. The low value obtained (-0.24) justifies the assumption of independent random variables. Thus, two statistical models (for G and ξ) has been developed starting from the relevant set of available experimental data. The parameters of the statistical models obtained are summarized in Table 2. In particular, the overall mean, the relevant coefficient of variation (CV), the overall standard deviation (σ), the within-class and between-class standard variations ($\sigma_W$ and $\sigma_B$) and the correlation index are reported. The obtained results show that overall mean values $\mu_G$ = 0.41 MPa and $\mu_\xi$ = 15.6% are very close to the nominal ones, moreover the within-class variability is significant lower than the between-class variability. Consequently, high correlation coefficients are obtained.

**Table 2**: ANOVA model II values for *G* and *ξ*

| | $\mu$ [MPa] | *CV* | $\sigma$ [MPa] | $\sigma_B$ [MPa] | $\sigma_W$ [MPa] | *IC* |
|---|---|---|---|---|---|---|
| *G* | 0.417 | 9.43% | 0.0394 | 0.0362 | 0.0155 | 0.845 |
| *ξ* | 0.157 | 7.36% | 0.0115 | 0.0105 | 0.0047 | 0.831 |

Figure 1 shows the experimental distributions of the batches tested and the calculated general distribution for *G* and *ξ*. According to these distributions, a procedure that randomly generate G and ξ values of bearings belonging to several batches having different sizes (number of isolators for each batch) has been developed.

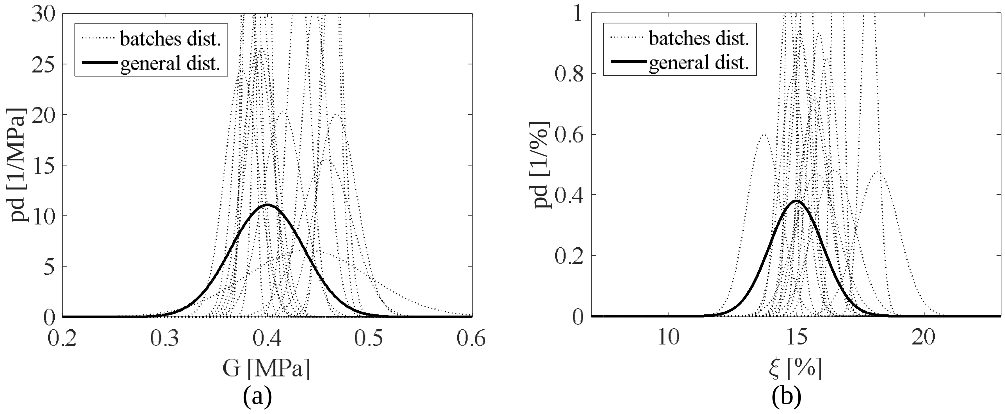


**Figure 1**: batch distributions and general distribution of $G$ (a) and $\xi$ (b)

## 2.3 Acceptance criteria

According to factory production control tests required by EN15129, the first seismic isolator and at least 20% of the following produced devices, chosen randomly for each type, shall be tested (section 8.2.4.1.4). The parameters measured in the tests cannot show variations larger than 20% with respect to the nominal value. No indications about consequences of a negative results of the FPCT are given by the code. In this work, it is conservatively assumed that if one of the tested isolators belonging to a batch is out of the FPCT limits the entire batch is considered non-conforming.

By generating batches of HDR bearings, according to the statistical model described in the previous section, not all the batches pass the test. Obviously, the isolators belonging to the subset of conforming batches have a smaller variability. The rate of non-conforming batches and the consequent variability reduction depends on the overall variability of the adopted statistical model and the admitted tolerance limits.

Table 3 reports the coefficient of variation of the two parameters($G$ and $\xi$) of the subset of conforming batches, obtained by considering a large number of sampled batch (10000) and simulating the production control test. It is interesting to observe that the result of the test is also influenced by the size of the batch. In fact, by passing from batches with 5 isolators to batches with 100 isolators, the coefficients of variation show a moderate reduction in both the cases while the number of non-conforming batches notably increase.

**Table 3**: FPCT effects on different batch size

| *Batch size* | 5 | 10 | 15 | 20 | 30 | 50 | 100 |
|---|---|---|---|---|---|---|---|
| $CV_G$ | 8.7% | 8.6% | 8.4% | 8.2% | 8.1% | 7.9% | 7.6% |
| $CV_\xi$ | 7.2% | 7.1% | 7.1% | 7.0% | 7.0% | 6.9% | 6.8% |
| Non-conforming batches | 4% | 6% | 8% | 9% | 11% | 15% | 19% |

## 3 UNCERTAINTIES INFLUENCE ON THE SEISMIC RESPONSE OF SEISMIC ISOLATED BUILDINGS

A case study of an isolated building with 24 high damping rubber bearing, designed according to the Italian code [3], has been analysed to assess the influence of the variability of the isolators properties on the seismic response. Incremental dynamic nonlinear analysis has been performed on both the reference model with nominal properties and models with varied isolators properties, sampled according to the statistical model defined in the previous paragraphs. For the analyses accounting for isolation-related uncertainty, a one-to-one association between the 20 earthquakes of each intensity level and the 20 varied models is chosen.

### 3.1 Case Study

The selected case study is a seismic isolated building placed in L'Aquila (Italy, Lon. 13.40, Lat. 42.35, PGA 0.26g for A-type soil and $T_r$ = 475*yr*), consisting of a reinforced concrete structure of 6 floors, used also in the RINTC's project. ([4][5][6][7]). The building is intended for residential use, characterized by a regular plan of 240 square meters per storey. The inter-storey height is 3.40m at the ground level and 3.05m at the upper levels. The structure is isolated by 24 HDNR bearings. The isolation characteristics are shown in Table 4, where $\Phi$ is the isolator diameter, $t_e$ is the total rubber thickness, $\xi$ is the rubber damping, $d_{\text{max,HDRB}}$ is the displacement design capacity, $T_{is}$ is the isolation period, $T_{fb}$ is the fixed base period, $\gamma_{max}$ is the maximum shear deformation and D/C are the different demand/capacity ratio. Figure 2 (b) shows the plant distribution of the isolator.

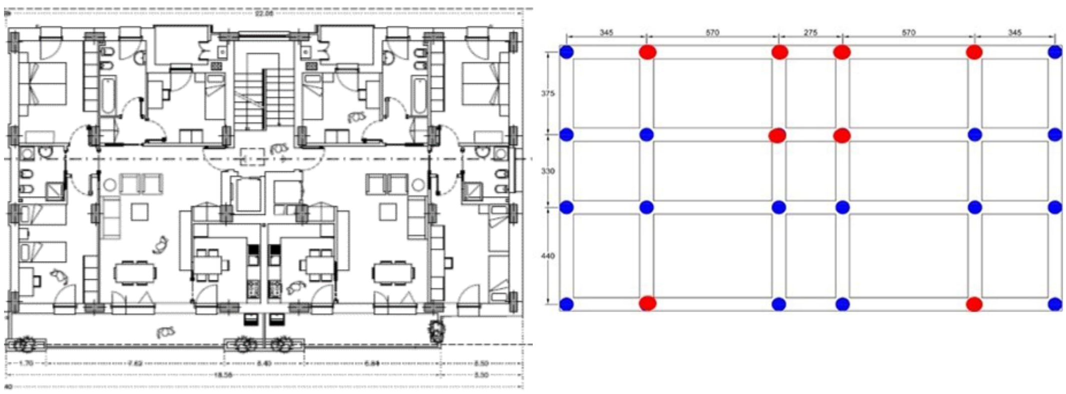

(a) (b)

**Figure 2**: model floor plan (a) and isolators distribution (b) (blue: ISO 550/154; red: ISO 600/150)

**Table 4**: isolation parameters and Demand/Capacity ratio

| HDRB $\Phi/t_e$ | $\xi$ (%) | $d_{\text{max,HDRB}}$ (mm) | $T_{is}$ (s) | $\gamma_{max}$ (-) | D/C shear | D/C compr. | D/C trac. | $T_{is}/T_{fb}$ | D/C drift |
|---|---|---|---|---|---|---|---|---|---|
| 550/154<br>600/150 | 15 | 300 | 2.46 | 1.71 | 0.86 | 0.97 | 0.33 | 3.46 | 0.21 |

A non-linear model has been implemented by using the OpenSees software [8]. The isolator response has been described by the model developed by Kumar et al [9], called HDR Bearing

Element, which adopts the bidirectional model proposed by Grant [10] for the shear behaviour. This model is able to describe the degradation of the bearing horizontal stiffness and damping due to the scragging and Mulllin's effect, which are essential for a reliable estimation of the dynamic response [11] [12]. The mechanical parameters for the shear behaviour has been calibrated on experimental tests. A lumped plasticity model for the bare frame and equivalent strut acting only in compression for the infill have been chosen for the superstructure. For further details on the modelling refers to the RINTC's project ([6][7][8]).

The seismic response is evaluated for 10 intensity levels of the seismic input (return period from 10 to 100000 years) with 20 ground motion per level, selected according the conditional spectrum approach (CS, [4]) and consistent to the magnitude-distance disaggregation of the site hazard. The intensity measure (IM) has been measured by the pseudo-acceleration spectral value for T = 3s (the nearest value to the isolation period [4]). Table 5 reports the intensity values for the 10 levels considered together with the mean annual frequency of exceedance per year in the building site (L'Aquila area).

**Table 5**: return period, mean annual frequency of exceedance per year and pseudo acceleration

| $T_r$ **[yrs]** | 10 | 50 | 100 | 250 | 500 | 1000 | 2500 | 5000 | 10000 | 10000 |
|---|---|---|---|---|---|---|---|---|---|---|
| $\nu$ | 0.0952 | 0.0198 | 0.0010 | 0.0040 | 0.0020 | 0.001 | 0.0004 | 0.0002 | 1E-04 | 1E-05 |
| ***Sa (T=3s)*** **[g]** | 0.002 | 0.011 | 0.031 | 0.062 | 0.11 | 0.177 | 0.271 | 0.384 | 0.576 | 1.053 |

## 3.2 Isolation variability sampling

In order to have consistency with analysis results without isolation-related uncertainties, in the generation procedure of batches mean values are assumed coincident with the design ones. Moreover, rounded values of the ANOVA models are assumed, as reported in Table 6. Table 7 and Table 8 show the generated values of $G$ and $\xi$ of each isolator (column data) and each batch (row data). Red values are related to the virtually tested isolators while the orange highlight values correspond to the non-conforming isolators (variation greater than ±20%). For this case study, 21 batches of 24 isolators are generated and checked: only one of them, displayed in the last row, is rejected because 2 out of 5 tested isolators do not respect the tolerance ±20% for what concern G (0.32÷0.48 MPa).

**Table 6**: ANOVA model II values for $G$ and $\xi$

| | $\mu_T$ [MPa] | $CV_T$ | $\sigma_T$ [MPa] | $\sigma_B$ [MPa] | $\sigma_W$ [MPa] | $IC$ |
|---|---|---|---|---|---|---|
| $G$ | **0.4** | **9%** | 0.036 | 0.0332 | 0.0139 | **0.85** |
| $\xi$ | **0.15** | **7%** | 0.0105 | 0.0097 | 0.0041 | **0.85** |

It is possible that some accepted isolators do not respect the tolerance limits (6 for $G$ and 1 for $\xi$) but they haven't been tested so their batch pass the virtual check. The $G$ distributions of each batch sampled is plotted in terms of probability density function to highlight the within- and the between-variability in Figure 3 (a). Because the within-variability is small, the rejected batches are usually characterized by a high number of non-conforming isolators, as shown in this example by the blue bell.

**Table 7**: *G* varied values

| G [MPA] | ISOLATION DEVICES 1 | 2 | 3 | 4 | 5 | 6 | 7 | 8 | 9 | 10 | 11 | 12 | 13 | 14 | 15 | 16 | 17 | 18 | 19 | 20 | 21 | 22 | 23 | 24 |
|---|---|---|---|---|---|---|---|---|---|---|---|---|---|---|---|---|---|---|---|---|---|---|---|---|
| STOCKS 1 | 0.400 | 0.384 | 0.397 | 0.401 | 0.408 | 0.415 | 0.412 | 0.398 | 0.409 | 0.389 | 0.403 | 0.416 | 0.388 | 0.400 | 0.422 | 0.405 | 0.415 | 0.406 | 0.389 | 0.389 | 0.391 | 0.381 | 0.398 | 0.388 |
| 2 | 0.431 | 0.438 | 0.432 | 0.417 | 0.422 | 0.416 | 0.428 | 0.429 | 0.429 | 0.427 | 0.407 | 0.438 | 0.419 | 0.447 | 0.414 | 0.445 | 0.396 | 0.415 | 0.432 | 0.416 | 0.424 | 0.422 | 0.427 | 0.436 |
| 3 | 0.385 | 0.394 | 0.403 | 0.391 | 0.420 | 0.370 | 0.429 | 0.398 | 0.423 | 0.385 | 0.404 | 0.387 | 0.422 | 0.423 | 0.420 | 0.396 | 0.376 | 0.384 | 0.396 | 0.401 | 0.409 | 0.404 | 0.414 | 0.405 |
| 4 | 0.403 | 0.403 | 0.410 | 0.392 | 0.381 | 0.404 | 0.394 | 0.396 | 0.426 | 0.388 | 0.401 | 0.386 | 0.392 | 0.405 | 0.400 | 0.384 | 0.417 | 0.385 | 0.431 | 0.411 | 0.384 | 0.408 | 0.421 | 0.422 |
| 5 | 0.409 | 0.427 | 0.412 | 0.418 | 0.398 | 0.408 | 0.422 | 0.426 | 0.432 | 0.414 | 0.434 | 0.391 | 0.434 | 0.432 | 0.411 | 0.407 | 0.410 | 0.421 | 0.416 | 0.424 | 0.412 | 0.418 | 0.398 | 0.419 |
| 6 | 0.437 | 0.464 | 0.450 | 0.430 | 0.451 | 0.405 | 0.484 | 0.439 | 0.416 | 0.431 | 0.413 | 0.438 | 0.427 | 0.427 | 0.444 | 0.434 | 0.418 | 0.421 | 0.435 | 0.465 | 0.412 | 0.431 | 0.424 | 0.419 |
| 7 | 0.452 | 0.437 | 0.436 | 0.460 | 0.443 | 0.430 | 0.453 | 0.443 | 0.442 | 0.444 | 0.446 | 0.452 | 0.411 | 0.435 | 0.451 | 0.415 | 0.449 | 0.468 | 0.433 | 0.443 | 0.426 | 0.455 | 0.431 | 0.442 |
| 8 | 0.391 | 0.398 | 0.415 | 0.408 | 0.424 | 0.397 | 0.403 | 0.432 | 0.416 | 0.423 | 0.388 | 0.422 | 0.419 | 0.442 | 0.411 | 0.413 | 0.404 | 0.403 | 0.421 | 0.409 | 0.426 | 0.399 | 0.422 | 0.408 |
| 9 | 0.378 | 0.367 | 0.376 | 0.387 | 0.386 | 0.378 | 0.383 | 0.374 | 0.390 | 0.376 | 0.369 | 0.350 | 0.384 | 0.366 | 0.385 | 0.373 | 0.393 | 0.377 | 0.395 | 0.385 | 0.368 | 0.385 | 0.381 | 0.374 |
| 10 | 0.405 | 0.421 | 0.444 | 0.430 | 0.439 | 0.427 | 0.438 | 0.436 | 0.435 | 0.429 | 0.418 | 0.449 | 0.431 | 0.447 | 0.429 | 0.419 | 0.441 | 0.398 | 0.441 | 0.420 | 0.422 | 0.441 | 0.434 | 0.416 |
| 11 | 0.430 | 0.442 | 0.433 | 0.450 | 0.455 | 0.430 | 0.471 | 0.447 | 0.441 | 0.445 | 0.440 | 0.429 | 0.451 | 0.464 | 0.437 | 0.457 | 0.434 | 0.436 | 0.479 | 0.448 | 0.460 | 0.435 | 0.461 | 0.447 |
| 12 | 0.381 | 0.376 | 0.360 | 0.367 | 0.375 | 0.370 | 0.355 | 0.370 | 0.368 | 0.382 | 0.407 | 0.363 | 0.373 | 0.387 | 0.392 | 0.385 | 0.363 | 0.385 | 0.375 | 0.387 | 0.367 | 0.398 | 0.377 | 0.371 |
| 13 | 0.431 | 0.425 | 0.427 | 0.446 | 0.421 | 0.416 | 0.428 | 0.422 | 0.428 | 0.457 | 0.427 | 0.408 | 0.401 | 0.448 | 0.430 | 0.417 | 0.441 | 0.437 | 0.407 | 0.415 | 0.441 | 0.415 | 0.443 | 0.424 |
| 14 | 0.385 | 0.403 | 0.403 | 0.412 | 0.439 | 0.394 | 0.429 | 0.395 | 0.379 | 0.415 | 0.395 | 0.419 | 0.392 | 0.408 | 0.398 | 0.412 | 0.388 | 0.384 | 0.379 | 0.408 | 0.410 | 0.414 | 0.421 | 0.394 |
| 15 | 0.355 | 0.344 | 0.355 | 0.344 | 0.341 | 0.345 | 0.335 | 0.363 | 0.319 | 0.350 | 0.357 | 0.345 | 0.359 | 0.336 | 0.330 | 0.342 | 0.330 | 0.347 | 0.347 | 0.344 | 0.364 | 0.361 | 0.374 | 0.341 |
| 16 | 0.422 | 0.404 | 0.423 | 0.411 | 0.429 | 0.404 | 0.428 | 0.436 | 0.419 | 0.441 | 0.403 | 0.406 | 0.420 | 0.419 | 0.394 | 0.427 | 0.439 | 0.390 | 0.405 | 0.421 | 0.423 | 0.432 | 0.395 | 0.425 |
| 17 | 0.413 | 0.394 | 0.398 | 0.402 | 0.391 | 0.408 | 0.400 | 0.385 | 0.418 | 0.421 | 0.414 | 0.410 | 0.394 | 0.402 | 0.427 | 0.425 | 0.397 | 0.407 | 0.397 | 0.408 | 0.376 | 0.391 | 0.407 | 0.400 |
| 18 | 0.390 | 0.402 | 0.416 | 0.399 | 0.413 | 0.400 | 0.424 | 0.396 | 0.396 | 0.411 | 0.410 | 0.408 | 0.409 | 0.426 | 0.412 | 0.403 | 0.419 | 0.392 | 0.403 | 0.409 | 0.420 | 0.402 | 0.433 | 0.410 |
| 19 | 0.473 | 0.454 | 0.450 | 0.453 | 0.446 | 0.443 | 0.447 | 0.465 | 0.483 | 0.463 | 0.512 | 0.450 | 0.483 | 0.450 | 0.451 | 0.470 | 0.475 | 0.478 | 0.461 | 0.476 | 0.473 | 0.470 | 0.506 | 0.462 |
| 20 | 0.407 | 0.420 | 0.392 | 0.428 | 0.429 | 0.393 | 0.417 | 0.417 | 0.411 | 0.416 | 0.426 | 0.406 | 0.418 | 0.425 | 0.401 | 0.393 | 0.400 | 0.402 | 0.412 | 0.386 | 0.400 | 0.406 | 0.400 | 0.427 |
| | 0.307 | 0.331 | 0.318 | 0.309 | 0.312 | 0.325 | 0.318 | 0.331 | 0.327 | 0.331 | 0.317 | 0.330 | 0.345 | 0.318 | 0.324 | 0.318 | 0.322 | 0.344 | 0.342 | 0.348 | 0.306 | 0.332 | 0.324 | 0.346 |

**Table 8**: $\xi$ varied values

| $\xi$ [-] | ISOLATION DEVICES 1 | 2 | 3 | 4 | 5 | 6 | 7 | 8 | 9 | 10 | 11 | 12 | 13 | 14 | 15 | 16 | 17 | 18 | 19 | 20 | 21 | 22 | 23 | 24 |
|---|---|---|---|---|---|---|---|---|---|---|---|---|---|---|---|---|---|---|---|---|---|---|---|---|
| STOCKS 1 | 0.150 | 0.149 | 0.143 | 0.145 | 0.147 | 0.143 | 0.142 | 0.153 | 0.152 | 0.144 | 0.144 | 0.148 | 0.143 | 0.145 | 0.145 | 0.147 | 0.148 | 0.145 | 0.153 | 0.146 | 0.141 | 0.143 | 0.140 | 0.147 |
| 2 | 0.168 | 0.175 | 0.180 | 0.166 | 0.177 | 0.173 | 0.167 | 0.167 | 0.170 | 0.175 | 0.172 | 0.170 | 0.169 | 0.164 | 0.176 | 0.167 | 0.169 | 0.164 | 0.168 | 0.178 | 0.176 | 0.170 | 0.185 | 0.172 |
| 3 | 0.132 | 0.143 | 0.135 | 0.142 | 0.138 | 0.141 | 0.142 | 0.143 | 0.142 | 0.136 | 0.135 | 0.142 | 0.141 | 0.138 | 0.136 | 0.141 | 0.144 | 0.140 | 0.140 | 0.137 | 0.144 | 0.142 | 0.139 | 0.139 |
| 4 | 0.138 | 0.144 | 0.147 | 0.148 | 0.145 | 0.145 | 0.148 | 0.142 | 0.139 | 0.148 | 0.144 | 0.144 | 0.150 | 0.144 | 0.143 | 0.144 | 0.146 | 0.143 | 0.148 | 0.147 | 0.147 | 0.149 | 0.151 | 0.147 |
| 5 | 0.147 | 0.150 | 0.148 | 0.145 | 0.145 | 0.149 | 0.151 | 0.150 | 0.149 | 0.144 | 0.147 | 0.154 | 0.151 | 0.147 | 0.149 | 0.146 | 0.150 | 0.157 | 0.146 | 0.155 | 0.142 | 0.149 | 0.139 | 0.153 |
| 6 | 0.161 | 0.154 | 0.157 | 0.160 | 0.163 | 0.167 | 0.163 | 0.165 | 0.160 | 0.165 | 0.163 | 0.161 | 0.166 | 0.165 | 0.161 | 0.165 | 0.163 | 0.163 | 0.167 | 0.166 | 0.162 | 0.162 | 0.159 | 0.164 |
| 7 | 0.162 | 0.155 | 0.161 | 0.163 | 0.156 | 0.155 | 0.163 | 0.159 | 0.168 | 0.166 | 0.166 | 0.157 | 0.157 | 0.155 | 0.158 | 0.155 | 0.159 | 0.159 | 0.155 | 0.147 | 0.154 | 0.154 | 0.156 | 0.164 |
| 8 | 0.140 | 0.127 | 0.131 | 0.138 | 0.132 | 0.128 | 0.138 | 0.135 | 0.132 | 0.137 | 0.132 | 0.135 | 0.140 | 0.135 | 0.136 | 0.133 | 0.131 | 0.127 | 0.129 | 0.138 | 0.133 | 0.137 | 0.128 | 0.126 |
| 9 | 0.160 | 0.164 | 0.164 | 0.158 | 0.155 | 0.160 | 0.158 | 0.163 | 0.161 | 0.168 | 0.160 | 0.159 | 0.161 | 0.158 | 0.162 | 0.169 | 0.159 | 0.159 | 0.169 | 0.154 | 0.157 | 0.164 | 0.157 | 0.172 |
| 10 | 0.160 | 0.171 | 0.164 | 0.150 | 0.165 | 0.158 | 0.161 | 0.159 | 0.161 | 0.167 | 0.160 | 0.162 | 0.168 | 0.159 | 0.164 | 0.161 | 0.159 | 0.156 | 0.166 | 0.155 | 0.158 | 0.157 | 0.154 | 0.160 |
| 11 | 0.147 | 0.146 | 0.142 | 0.143 | 0.135 | 0.145 | 0.139 | 0.143 | 0.136 | 0.140 | 0.140 | 0.143 | 0.136 | 0.141 | 0.143 | 0.139 | 0.143 | 0.142 | 0.144 | 0.144 | 0.145 | 0.142 | 0.140 | 0.142 |
| 12 | 0.163 | 0.173 | 0.167 | 0.156 | 0.168 | 0.160 | 0.160 | 0.169 | 0.159 | 0.165 | 0.162 | 0.162 | 0.167 | 0.164 | 0.162 | 0.171 | 0.159 | 0.159 | 0.166 | 0.162 | 0.165 | 0.161 | 0.159 | 0.160 |
| 13 | 0.153 | 0.141 | 0.139 | 0.146 | 0.145 | 0.148 | 0.143 | 0.150 | 0.145 | 0.145 | 0.145 | 0.143 | 0.147 | 0.142 | 0.145 | 0.145 | 0.146 | 0.145 | 0.140 | 0.146 | 0.141 | 0.142 | 0.144 | 0.150 |
| 14 | 0.154 | 0.159 | 0.151 | 0.150 | 0.151 | 0.151 | 0.151 | 0.150 | 0.150 | 0.149 | 0.145 | 0.149 | 0.145 | 0.145 | 0.145 | 0.143 | 0.144 | 0.148 | 0.151 | 0.157 | 0.148 | 0.148 | 0.143 | 0.152 |
| 15 | 0.137 | 0.136 | 0.127 | 0.136 | 0.135 | 0.137 | 0.134 | 0.139 | 0.137 | 0.142 | 0.130 | 0.139 | 0.136 | 0.129 | 0.132 | 0.134 | 0.134 | 0.143 | 0.136 | 0.134 | 0.137 | 0.142 | 0.140 | 0.129 |
| 16 | 0.153 | 0.153 | 0.145 | 0.144 | 0.146 | 0.142 | 0.149 | 0.150 | 0.152 | 0.156 | 0.146 | 0.151 | 0.148 | 0.144 | 0.151 | 0.146 | 0.148 | 0.151 | 0.149 | 0.146 | 0.142 | 0.142 | 0.146 | 0.146 |
| 17 | 0.147 | 0.144 | 0.143 | 0.142 | 0.139 | 0.139 | 0.135 | 0.147 | 0.142 | 0.140 | 0.136 | 0.141 | 0.138 | 0.143 | 0.134 | 0.141 | 0.143 | 0.135 | 0.137 | 0.134 | 0.145 | 0.139 | 0.140 | 0.136 |
| 18 | 0.143 | 0.141 | 0.142 | 0.143 | 0.141 | 0.139 | 0.143 | 0.138 | 0.139 | 0.132 | 0.142 | 0.139 | 0.139 | 0.131 | 0.145 | 0.141 | 0.144 | 0.139 | 0.146 | 0.143 | 0.136 | 0.137 | 0.137 | 0.140 |
| 19 | 0.135 | 0.135 | 0.142 | 0.132 | 0.134 | 0.136 | 0.130 | 0.140 | 0.134 | 0.143 | 0.138 | 0.132 | 0.139 | 0.128 | 0.137 | 0.137 | 0.136 | 0.135 | 0.129 | 0.140 | 0.133 | 0.138 | 0.130 | 0.131 |
| 20 | 0.156 | 0.153 | 0.153 | 0.152 | 0.154 | 0.157 | 0.159 | 0.161 | 0.152 | 0.160 | 0.149 | 0.157 | 0.154 | 0.156 | 0.158 | 0.152 | 0.163 | 0.159 | 0.154 | 0.157 | 0.162 | 0.159 | 0.154 | 0.162 |
| | 0.142 | 0.144 | 0.142 | 0.140 | 0.141 | 0.142 | 0.139 | 0.143 | 0.143 | 0.148 | 0.145 | 0.143 | 0.139 | 0.143 | 0.141 | 0.146 | 0.139 | 0.146 | 0.142 | 0.146 | 0.138 | 0.142 | 0.147 | 0.144 |

Once $G$ and $\xi$ values of each isolator of each batch have been generated, an automatic procedure has been developed to calibrate the Grant model according to the obtained sampled values of stiffness and damping at the third cycle and at the designed deformation. An example of the cyclic behaviour for the nominal parameters (blue) and for two varied parameters (red and yellow) is shown in Figure 3 (b).

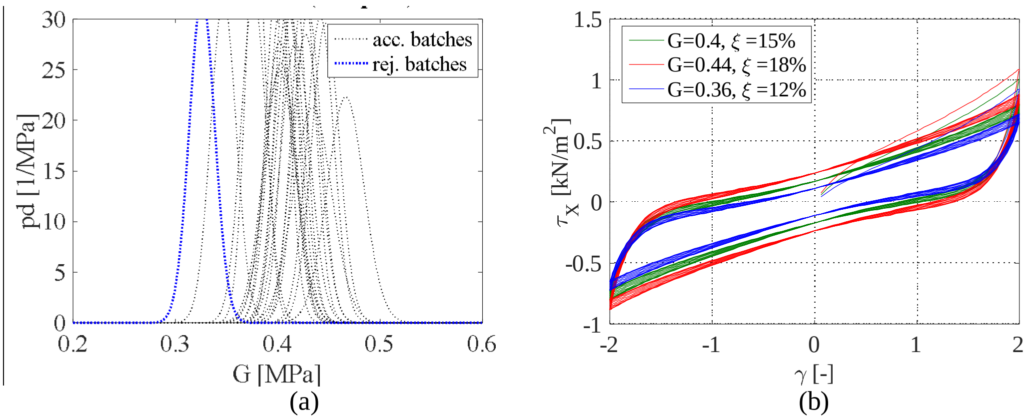


**Figure 3**: probability density functions of sampled batches (a) and hysteretic cycle comparison between nominal and varied parameters (b)

## 3.3 Influence of uncertainties on the seismic performance

Figure 5 shows the analysis results in terms ofdemand/capacity ratio (D/C) related to the shear deformation of the isolation system and the superstructure displacement in the two directions X and Y (relative top floor displacement with respect to the isolated base). In particular, demand values are evaluated caring out multi-stripe nonlinear analyses by considering 20 ground motion records for 10 intensity measure (IM) levels . Based on indications reported in the scientific literature (ref) the capacity of the bearings in terms of shear deformation is assumed equal to 350%. For the superstructure capacity, push over analyses are performed on the fixed-base superstructure and displacements corresponding to the 50% of strength reduction are calculated. Results are 504mm for the X direction and 273 mm for the Y direction. Blue marks reported in Figure 5 concern the analyses with nominal properties, while the red ones concern the analyses with the varied parameters of bearings.

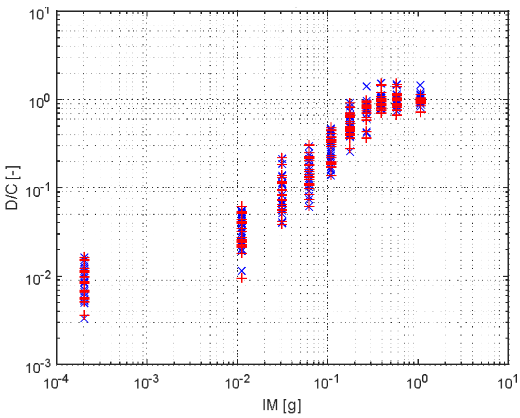


**Figure 4**: comparison between nominal (blue) and varied models (red) for $\gamma$

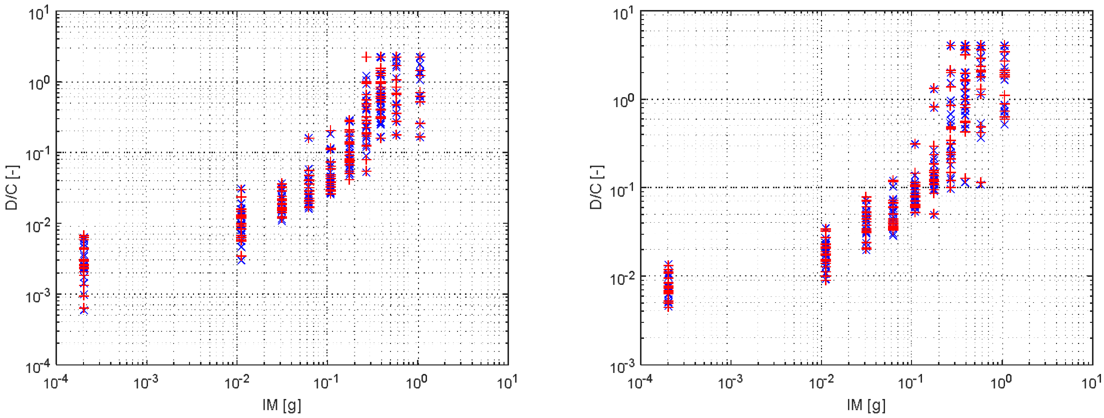


(a) (b)

**Figure 5**: comparison between nominal (blue) and varied models (red) for Delta X (a) and Delta Y (b) D/C

Results shows that the variability of the isolators properties does not influence significantly the response of the isolated structure, with respect to the influence of the seismic input variability (record-to-record variability). To better understand how the variability of *G* and *ξ* influences the response, Table 9,

Table ~~10~~ display the percentage variations of the considered response parameters for each non-linear time history analysis (percentage variations in Y direction, which are similar to the X direction, are not reported for space reason). The last two columns report the mean properties of the batch. Considering only the analysis where there are no-collapses (boxes not in orange), the variations are very low (almost all lower than the acceptance limit ±20%). Only one varied model (n°15), where G and ξ are reduced respectively of 13.3% and of 9.6%, shows greater increases in terms of shear deformation (up to +41%). The same model, on the other hand, also shows the highest reduction in terms of maximum drift in X and Y direction.

**Table 9**: percentage variations of the shear deformation between nominal and varied models

| | **IM1** | **IM2** | **IM3** | **IM4** | **IM5** | **IM6** | **IM7** | **IM8** | **IM9** | **IM10** | ***G*** | ***ξ*** |
|---|---|---|---|---|---|---|---|---|---|---|---|---|
| **1** | 7% | 1% | 5% | 1% | 0% | 7% | 4% | 3% | -2% | 0% | 0.0% | -2.7% |
| **2** | -3% | 0% | -5% | -16% | -11% | -1% | -3% | -2% | -3% | -9% | 6.3% | 14.4% |
| **3** | 5% | 4% | 2% | 2% | 15% | 2% | 0% | 0% | 63% | -1% | 0.4% | -6.9% |
| **4** | -5% | -1% | 1% | 1% | 2% | 0% | 1% | 29% | 1% | -1% | 0.5% | -3.1% |
| **5** | -5% | -2% | -3% | -1% | -4% | -3% | -2% | -2% | -1% | -1% | 4.1% | -1.0% |
| **6** | 15% | -9% | 2% | -7% | -4% | -3% | 2% | 40% | -3% | -8% | 8.5% | 8.3% |
| **7** | 14% | 0% | 2% | -16% | -4% | -11% | -2% | -9% | -3% | -3% | 10.4% | 5.7% |
| **8** | 9% | 8% | 6% | 7% | 11% | 5% | 1% | 3% | -15% | -18% | 3.1% | -11.1% |
| **9** | 2% | -1% | 0% | 1% | -4% | -6% | 2% | 0% | 3% | -32% | -5.4% | 7.6% |
| **10** | -9% | -16% | 0% | -4% | -3% | -8% | -6% | -8% | -1% | 0% | 7.4% | 7.1% |
| **11** | 1% | -14% | -5% | -6% | -7% | 1% | -14% | -3% | -11% | -4% | 11.7% | -5.6% |
| **12** | 4% | -1% | -2% | -1% | -2% | -1% | 1% | 1% | 2% | 0% | -5.9% | 8.9% |
| **13** | -7% | -1% | 6% | -6% | -2% | -3% | -8% | -2% | -20% | 0% | 6.8% | -3.5% |
| **14** | 2% | -1% | 0% | 1% | -1% | 0% | -35% | -2% | 1% | -33% | 0.8% | -0.6% |
| **15** | -8% | 17% | 41% | 16% | 33% | 22% | 4% | 4% | 10% | 6% | -13.3% | -9.6% |
| **16** | 2% | 0% | 0% | 1% | -2% | -5% | -3% | 28% | -26% | -12% | 4.3% | -1.5% |
| **17** | 8% | -5% | 4% | 5% | 5% | 4% | 0% | 1% | -3% | 0% | 0.9% | -6.6% |
| **18** | -6% | 1% | 2% | 0% | 3% | 0% | -2% | 0% | -2% | -23% | 2.1% | -6.7% |
| **19** | -1% | -12% | 0% | -1% | -5% | -4% | -5% | -21% | -5% | -3% | 16.6% | -9.9% |
| **20** | 1% | -7% | -9% | -8% | -4% | -3% | -1% | -1% | 1% | 0% | 2.4% | 4.3% |

**Table 10**: percentage variations of the superstructure displacement (X dir) between nominal and varied models

| | IM1 | IM2 | IM3 | IM4 | IM5 | IM6 | IM7 | IM8 | IM9 | IM10 | *G* | *ξ* |
|---|---|---|---|---|---|---|---|---|---|---|---|---|
| **1** | -5% | -2% | 2% | 0% | -2% | 7% | 6% | 14% | 2% | 0% | 0.0% | -2.7% |
| **2** | -5% | 23% | 8% | 10% | 7% | 1% | -9% | 135% | 0% | 0% | 6.3% | 14.4% |
| **3** | -11% | -5% | -6% | -2% | -1% | 19% | 6% | 0% | -62% | 0% | 0.4% | -6.9% |
| **4** | -3% | -2% | -1% | -1% | 1% | 2% | 9% | 3% | 0% | 2% | 0.5% | -3.1% |
| **5** | 13% | 2% | 5% | 5% | 3% | -3% | 0% | 5% | -2% | 0% | 4.1% | -1.0% |
| **6** | 17% | 11% | 2% | 27% | 13% | 9% | -23% | -2% | 0% | 7% | 8.5% | 8.3% |
| **7** | 26% | 23% | 19% | 6% | 18% | -5% | 5% | -55% | 0% | 0% | 10.4% | 5.7% |
| **8** | -6% | 3% | -4% | 10% | 6% | 7% | 68% | 128% | -33% | 2% | 3.1% | -11.1% |
| **9** | 2% | -2% | -3% | -3% | -9% | -7% | 4% | -35% | 0% | 24% | -5.4% | 7.6% |
| **10** | 27% | 14% | 19% | 5% | 10% | 13% | -6% | -2% | 0% | -11% | 7.4% | 7.1% |
| **11** | 8% | 5% | 6% | 11% | -3% | 12% | -12% | 28% | 0% | 15% | 11.7% | -5.6% |
| **12** | -7% | -3% | -1% | -1% | -2% | -10% | -12% | -6% | -6% | 0% | -5.9% | 8.9% |
| **13** | 19% | -4% | 5% | 2% | 7% | 9% | 3% | 8% | 14% | 12% | 6.8% | -3.5% |
| **14** | 1% | 1% | 1% | 0% | 1% | 1% | 0% | 17% | -62% | 105% | 0.8% | -0.6% |
| **15** | -16% | -16% | 15% | -14% | -4% | -19% | 28% | -4% | 255% | 0% | -13.3% | -9.6% |
| **16** | 11% | 5% | 4% | 1% | 4% | 7% | 7% | -2% | 97% | 1% | 4.3% | -1.5% |
| **17** | -5% | -15% | -2% | -3% | -1% | 4% | 8% | 0% | 1% | -16% | 0.9% | -6.6% |
| **18** | 6% | 3% | -5% | -2% | 3% | 13% | 16% | 0% | 0% | 72% | 2.1% | -6.7% |
| **19** | 11% | 11% | 6% | 12% | 24% | 40% | 78% | 27% | 0% | 0% | 16.6% | -9.9% |
| **20** | 6% | 20% | -4% | 2% | 4% | 0% | 1% | 7% | 0% | 0% | 2.4% | 4.3% |

Very high value of percentage variations for the analysis with collapse (boxes in orange) are not associated to the isolators variability. They are instead caused by the stop of the analysis when one of the response parameter reach a demand > 2 times the capacity.

The seismic performance is also measured identifying the number of collapses of the isolation system for the different seismic intensities. In particular, besides the shear failure and superstructure collapse (X and Y direction) according to capacity previous defined, also the cavitation (deformation of 50% in traction) and buckling (axial compression load > critical buckling load for more than 50% of the base isolators simultaneously) collapse mechanisms of the isolators are considered. Collapse results are presented in Figure 6. The differences of the number and type of collapses for the model with nominal parameters and the one with varied parameters are negligible in terms of number collapse, only collapse modalities slightly change.

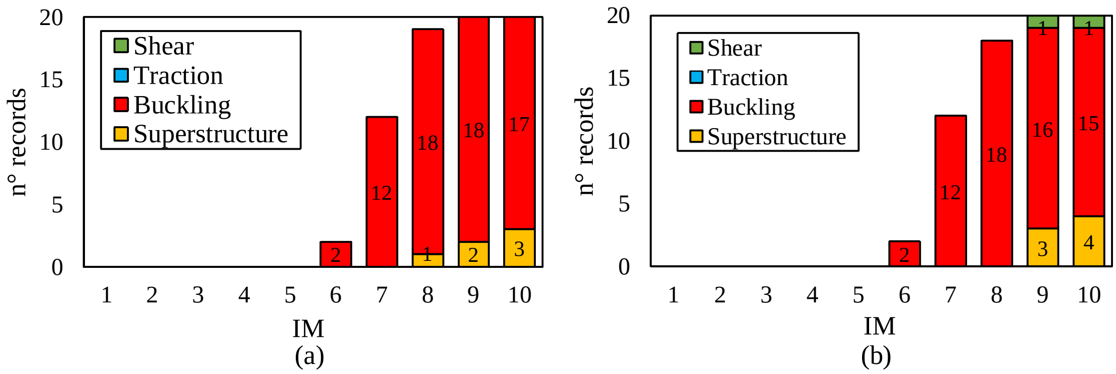


**Figure 6**: number and type of collapse for nominal model (a) and varied models (b)

## 4 CONCLUSION

The statistical processing of the experimental data supporting this study provided the following results: (i) the considered quantities ($G$ and $\xi$) can be considered not correlated; (ii) both quantities show experimental mean values very close to the nominal values; (iii) the variation coefficients are limited for both quantities (9% and 7% respectively for $G$ and $\xi$). Therefore, the data confirm that the production of elastomeric seismic isolators is quite reliable and so characterized by a low probability of non-compliance in the FPCT.

Moreover, results of numerical analyses carried out on isolated building showed that the influence of this limited variability of the isolator properties on the response of the isolated structure is very low compared to the influence of the seismic input variability (record-to-record variability). Consequently also the number collapses does not change significantly, only collapse modalities slightly change

## REFERENCES

[1] European Committee for Standardization. *EN 15129:2010 - Antiseismic devices*, Brussels, Belgium, 2010.

[2] Kutner M.H. [et al.]. *Applied linear statistical models*.-5th ed. (McGraw-Hill/Irwin series Operations and decision sciences)

[3] D.M Infrastrutture del 14 gennaio 2008. Nuove norme tecniche per le Costruzioni.

[4] Iervolino, I., Spillatura, A and Bazzurro, P. RINTC Project - Assessing the (implicit) seismic risk of code-conforming structures in Italy. *COMPDYN 2017*, Papadrakakis, M., Fragiadakis, M. (eds.) Rhodes Island, Greece, 15–17 June 2017.

[5] Camata, G., Celano, F., De Risi, M. T., Franchin, P., Magliulo, G., Manfredi, V., Masi, A., Mollaioli, F., Noto, F., Ricci, P., Spacone, E., Terrenzi, M., Verderame, G. (2017). RINTC Project - Nonlinear dynamic analyses of italian code-conforming reinforced concrete buildings for risk of collapse assessment. *COMPDYN 2017*, M. Papadrakakis, M. Fragiadakis (eds.) Rhodes Island, Greece, 15–17 June 2017.

[6] Cardone, D., Conte, N., Dall'Asta A., Di Cesare, A., Flora, A., Leccese, G., Mossucca, A., Micozzi, F., Ponzo, F. C., Ragni L. (2017). RINTC Project - Nonlinear analyses of Italian code-conforming base-isolated buildings for risk of collapse assessment. *COMPDYN 2017*, M. Papadrakakis, M. Fragiadakis (eds.) Rhodes Island, Greece, 15–17 June 2017.

[7] Franchin, P., Mollaioli, F., Noto F. (2017). RINTC Project - Influence of structure-related uncertainties on the risk of collapse of italian code-conforming reinforced concrete buildings. COMPDYN 2017, M. Papadrakakis, M. Fragiadakis (eds.) Rhodes Island, Greece, 15–17 June 2017

[8] McKenna F. (2011) OpenSees: a framework for earthquake engineering simulation, Computing in Science & Engineering 13.4: 58-66, (http://opensees.berkeley.edu).

[9] Kumar M., Whittaker A. e Constantinou M. (2014). An advanced numerical model of elastomeric seismic isolation bearings. *Earthquake Engineering & Structural Dynamics* 43(13):1955-1974.

[10] Grant DN, Fenves GL, Whittaker AS. Bidirectional modeling of high-damping rubber bearings. *Journal of Earthquake Engineering* 2004, **8**(1):161-185.

[11] Tubaldi E, Ragni L, Dall'Asta A, Ahmadi H, Muhr A. Stress softening behaviour of HDNR bearings: modelling and influence on the seismic response of isolated structures. *Earthq Eng Struct Dyn* 2017. http://dx.doi.org/10.1002/eqe.2897.

[12] Ragni, L., Tubaldi, E., Dall'Asta, A., Ahmadi, H., Muhr, A. (2018) Biaxial shear behaviour of HDNR with Mullins effect and deformation-induced anisotropy. Engineering Structures, 154, pp. 78-92. 2-s2.0-85033562862 WOS:000417664300007